Thermochimica Acta, 239 (1994) 253–268
Elsevier Science B.V., Amsterdam
SSDI 0040-6031(93)01653-K

Mössbauer spectroscopic and d.c. electrical conductivity study of the thermal decomposition of some iron(II) dicarboxylates [1]

A.K. Nikumbh [a,*], M.M. Phadke [a], S.K. Date [b] and P.P. Bakare [b]

[a] *Department of Chemistry, University of Poona, Ganeshkhind, Pune-411 007, India*
[b] *Physical Chemistry Division, National Chemical Laboratory, Pune-411 008, India*

(Received 8 June 1993; in final form 16 November 1993)

Abstract

The thermal decomposition of ferrous fumarate half hydrate, $FeC_4H_2O_4 \cdot 0.5H_2O$ and ferrous tartrate one and a half hydrate, $FeC_4H_4O_6 \cdot 1.5H_2O$ have been studied by two probe direct current electrical conductivity measurements under the atmospheres of static air and dynamic dry nitrogen. The products at each decomposition stage have been characterized by infrared spectroscopy, X-ray powder diffraction Mössbauer spectroscopy and gas chromatography. The change in the oxidation state of iron ion is clearly followed through the course of decomposition via the changes in the isomer shift and quadrupole splittings. The formation of intermediates such as FeO, Fe_3O_4, γ-Fe_2O_3 and α-Fe_2O_3 are also discussed and the results of the Mössbauer measurements are correlated with the thermal analysis of these dicarboxylates.

INTRODUCTION

Iron oxides have great technical importance (catalysis, pigments, gas sensors, electronic components, etc.). For this reason, their chemical and structural properties have been the subject of numerous studies. Also, the experimental conditions for the preparation of various iron oxides have been extensively investigated.

The thermal decomposition of iron(II) oxalate dihydrate has been studied by various workers using differential thermal analysis and thermogravimetric analysis, and also surface area measurements [1–19]. These indicate that reaction occurs in two ranges of temperature, approximately 150–250 and 300–390°C. The reactions occurring in the lower temperature range have been shown to be very sensitive to the composition of the atmosphere in which they were carried out, small quantities of oxygen in an otherwise inert atmosphere giving rise to exothermic differential thermal analysis peaks from oxidation of the anhydrous iron(II) oxalate initially formed.

* Corresponding author.

[1] Part 2 of the series: for Part 1 see ref. 48.

Although thermal decomposition of bivalent metal carboxylates has been extensively investigated [16–24], there has been little study of iron(II) carboxylates except for iron(II) oxalate [1–19]. Many iron(II) carboxylates are unstable when they are in contact with air. It was indicated that the decomposition process of iron(II) oxalate is very complicated mainly due to the variable valence of the iron.

Interest has recently been shown in the use of Mössbauer spectroscopic techniques in the study of solid-state decomposition of iron(II) oxalate, formate, gluconate and malonate [25–37]. The present work was undertaken (a) to investigate the formation of iron oxides during the thermal decomposition of $FeC_4H_2O_4 \cdot 0.5H_2O$ and $FeC_4H_4O_6 \cdot 1.5H_2O$ and (b) to obtain some information about the structural properties of iron oxides formed. The phase analysis and structural characterization were performed using ^{57}Fe Mössbauer spectroscopy, d.c. electrical conductivity measurements and X-ray diffraction studies.

EXPERIMENTAL

Ferrous fumarate half hydrate ($FeC_4H_2O_4 \cdot 0.5H_2O$) and ferrous tartrate one and a half hydrate ($FeC_4H_4O_6 \cdot 1.5H_2O$) were prepared using the methods described previously [24, 25]. Elemental analyses were made in wt% for $FeC_4H_2O_4 \cdot 0.5H_2O$ (C, 26.87 (26.83); H, 1.60 (1.67); Fe, 31.4 (31.21) and for $FeC_4H_4O_6 \cdot 1.5H_2O$ (C, 20.53 (20.79); H, 4.02 (4.11); Fe, 28.0 (27.4)) where the values in parentheses are calculated ones. The IR spectra showed frequencies corresponding to carboxylate group, hydroxyl group, metal–oxygen, etc. The bidentate linkage of the fumarate or tartrate group with the metal was confirmed on the basis of the difference between the antisymmetric and symmetric stretching frequencies [38]. The X-ray diffraction pattern showed that the sample was polycrystalline in nature and comparable with data reported for fumarate [24] and tartrate [25]. The presence of water of crystallization was confirmed on the basis of the thermal analysis curves. The compounds $FeC_4H_2O_4 \cdot 0.5H_2O$ and $FeC_4H_4O_6 \cdot 1.5H_2O$ have a magnetic moment 4.89 B.M. and 4.96 B.M. respectively, which indicates that the compounds have free spin with sp^3d^2 hybridization.

The procedures used for the measurements of thermal analyses (simultaneous TGA, DTA and DTG), direct current electrical conductivity, infrared spectra, X-ray powder diffraction and gas–liquid chromatography were similar to those reported earlier [1, 23–25].

For the Mössbauer study, the samples were heated isothermally in a silica boat at different temperatures for 1 h in a controlled temperature furnace under an atmosphere of static air or dynamic dry nitrogen. These isothermal samples were kept in a vacuum desiccator and removed at the time of measurement. The constant acceleration Mössbauer spectrometer (Austin

Science S-600) was used to record the Mössbauer data in conjunction with a 10 mC ^{57}Co in rhodium source. The spectrometer was calibrated using a natural iron foil. All the spectra were recorded at 298 ± 2 K. A sample containing approximately 10 mg cm^{-2} of natural iron was taken for each measurement. The values of isomer shift have been reported with respect to natural iron. The uncertainties in isomer shift, quadrupole splitting and internal magnetic field values are ± 0.02 mm s^{-1}, ± 0.03 mm s^{-1} and ± 5 kOe respectively.

RESULTS AND DISCUSSION

Thermal decomposition processes of ferrous fumarate half hydrate

The plot of log σ versus T^{-1} in Fig. 1(a) showed an increase in σ from 40 to 85°C and a decrease up to 160°C (region B) for the dehydration step. The isothermally heated $FeC_4H_2O_4 \cdot 0.5H_2O$ sample under this atmosphere at 110°C did not have any H–OH bands in the IR spectrum. Elemental analysis agreed well with the anhydrous compound $FeC_4H_2O_4$ and the X-ray diffraction pattern was less crystalline than the parent compound $FeC_4H_2O_4 \cdot 0.5H_2O$ [24]. The σ value steadily increased from 160 and 226°C (region C), and the IR spectrum of the isothermally heated $FeC_4H_2O_4 \cdot 0.5H_2O$ sample at 220°C showed a decrease in intensity of

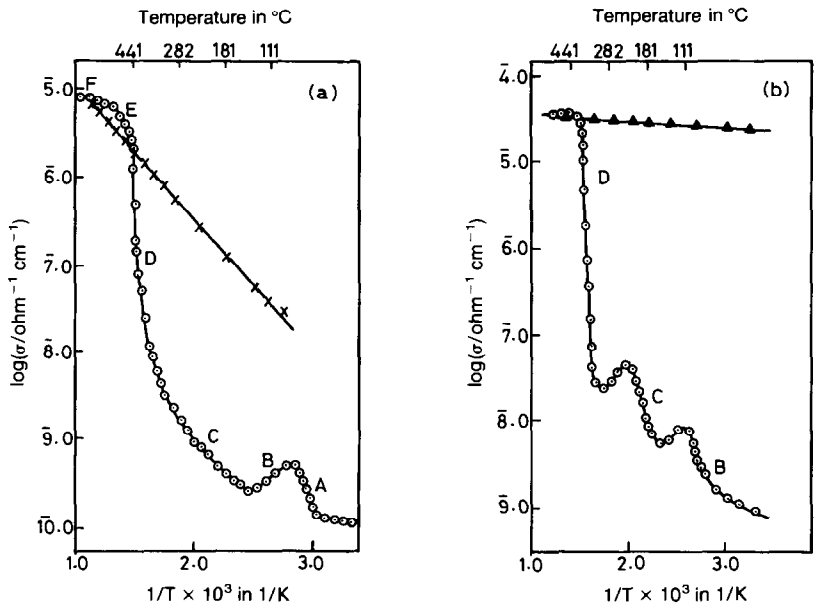

Fig. 1. Plot of log σ vs. T^{-1} for $FeC_4H_2O_4 \cdot 0.5H_2O$ during decomposition in (a) static air and (b) dynamic dry nitrogen atmosphere: ⊙, during decomposition; ×, cooling cycle for α-Fe_2O_3; ▲, cooling cycle for Fe_3O_4.

coordinated carboxylate bands; in addition, bands at 390 cm^{-1} (s) and 360 cm^{-1} (m) occurred for metal–oxygen stretching frequencies due to the presence of iron oxide [38]. The X-ray diffraction pattern of this isothermally heated sample showed the structure to be polycrystalline in nature, and peaks corresponding to both $FeC_4H_2O_4$ and FeO were observed. Even though a tendency for a sharp increase in σ was observed at region D (226–320°C), the characteristic high value of Fe_3O_4 (3.0 Mho cm^{-1}) could be obtained under dynamic conditions. However, the X-ray diffraction studies confirmed that mainly Fe_3O_4 was formed at this temperature. The intermediate obtained in region E (320–390°C) was mainly γ-Fe_2O_3 with traces of Fe_3O_4. The X-ray diffraction was generally broad, having peaks corresponding mainly to γ-Fe_2O_3 and traces of Fe_3O_4. The IR spectrum of the parent sample heated at 350°C showed no bands due to coordinated carboxylate, but strong and broad bands of Fe–O stretching frequencies were observed. This part of the graph is followed by region F (i.e. above 400°C) corresponding to the complete transformation of γ-Fe_2O_3 to α-Fe_2O_3.

A comparison of conventional thermal analysis [24] in static air, with conductivity analysis in static air, of $FeC_4H_2O_4 \cdot 0.5H_2O$ shows that the conductivity analysis gives a much more detailed view of the decomposition process. TGA shows a continuous mass loss between 60 and 400°C. DTA and DTG give an endothermic peak at 70°C corresponding to the dehydration of the half hydrate complex, a broad exothermic peak (at about 290°C) between 250 and 380°C corresponding to the oxidative decomposition of $FeC_4H_2O_4$ to the crystalline α-Fe_2O_3.

The Mössbauer spectra of the original sample and product at each decomposition stage are shown in Fig. 2 and the spectral parameters are summarized in Table 1. The Mössbauer spectrum of $FeC_4H_2O_4 \cdot 0.5H_2O$ (curve (a) in Fig. 2) gave two absorption bands with equal width and intensity, indicating that Fe^{2+} is in a one ion site, probably in an octahedral environment. The isomer shift and quadrupole splitting at room temperature are respectively 1.21 and 2.38 mm s^{-1}. The values of isomer shift and quadrupole splittng were in good agreement with those in the literature [5]. $FeC_4H_2O_4 \cdot 0.5H_2O$ is, therefore, a spin-free compound with some interaction between the Fe^{2+} ion and the asymmetrically arranged fumarate groups. The Mössbauer spectrum of anhydrous fumarate (curve (b) in Fig. 2) showed two absorptions, but they were broad and had different widths. The broadening reflects an unstable environment around Fe^{2+}, which is consistent with the fact that the anhydrous fumarate was in the amorphous state. It should be noted here that sample of $FeC_4H_2O_4$ stored in a desiccator for more than 7 days shows a similar Mössbauer spectrum. These observations indicate that a slow oxidation of the anhydrous material could not be detected.

The Mössbauer spectrum of a sample of $FeC_4H_2O_4 \cdot 0.5H_2O$ heated isothermally at 220°C (curve (c) in Fig. 2) showed two asymmetric peaks

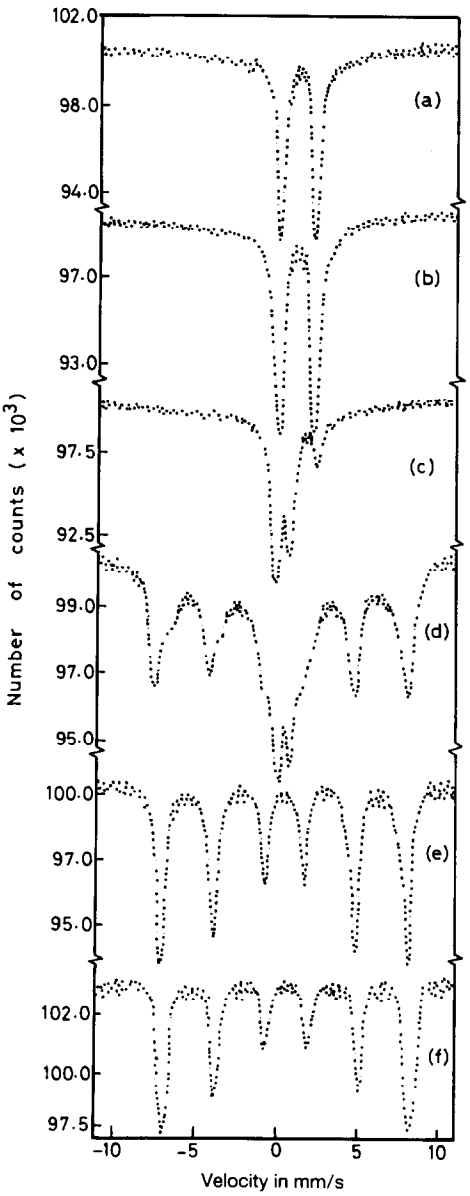

Fig. 2. Room-temperature Mössbauer spectra of (a) $FeC_4H_2O_4 \cdot 0.5H_2O$ and its products at (b) 100°C, (c) 220°C, (d) 300°C, (e) 350°C, (f) 410°C in static air.

separated by a distance of 0.7 mm s^{-1} and the more acute spectrum indicated an apparent Fe^{2+} quadrupole doublet. In addition to this a Mössbauer peak at 2.5 mm s^{-1} indicates the presence of a small amount of $FeC_4H_2O_4$. The values of isomer shift and quadrupole splitting were near the published data for FeO [39]. It has been observed [39] that the

TABLE 1

Mössbauer parameters [a] of $FeC_4H_2O_4 \cdot 0.5H_2O$ and its products at each decomposition stage; Mössbauer measurements were carried out at room temperature (25°C)

Atmosphere	Temperature ranges/°C	Region	Predicted products	Isomer shift/mm s^{-1} [b]	Quadrupole splitting/mm s^{-1} [c]	Internal magnetic field/kOe [d]
Static air	25	A	$FeC_4H_2O_4 \cdot 0.5H_2O$	1.21	2.38	
	60–160	B	$FeC_4H_2O_4$	1.25	2.65	
	160–226	C	$FeO + FeC_4H_2O_4$	0.68	0.55	
	226–320	D	Fe_3O_4	0.46	0.80	480
	320–390	E	γ-Fe_2O_3	0.24		492
	Above 410	F	α-Fe_2O_3	0.31	0.20	512
Dynamic dry nitrogen	25	A	$FeC_4H_2O_4 \cdot 0.5H_2O$	1.25	1.84	
	65–160	B	$FeC_4H_2O_4$	1.23	2.45	
	160–280	C	$FeO + FeC_4H_4O_4$	0.63	0.65	
	280–440	D	Fe_3O_4	0.48	0.76	482

[a] With respect to natural iron foil. [b] Values $\pm$ 0.02 mm s^{-1}. [c] Values $\pm$ 0.03 mm s^{-1}. [d] Values $\pm$ 5.0 kOe.

appearance of an asymmetric peak height lead to the identification of the major peaks as arising from quadrupole split Fe^{2+} and the distortion zero velocity as arising from a small amount of Fe^{3+}. The detailed shape and temperature dependence of the Mössbauer spectra of FeO have been described [39]. However, the present data may not be very accurate because of instrumental difficulties. We therefore conclude that, although decomposition occurred, the thermal energy at this temperature was much lower than the activation energy required for migration of the active material into the lattice sites of Fe_2O_3 (even at 270°C). The appearance of a central peak at 0.00 mm s^{-1} is due to oxidation of some of atoms on the surface of the solid to the tervalent state, so that a spin free Fe^{3+} Mössbauer spectra appears. Here we tentatively assume that the sample obtained at 220°C is a mixture of FeO and $FeC_4H_2O_4$, and that a small amount of Fe^{3+} is also formed. The X-ray diffraction pattern and IR spectrum showed the formation of FeO with traces of $FeC_4H_2O_4$.

For the $FeC_4H_2O_4 \cdot 0.5H_2O$ sample heated isothermally at 300°C, the Mössbauer spectrum consisted of several peaks (curve (d) in Fig. 2), in which, in addition to the doublet due to low-spin Fe^{2+}, the emergence of a sextet has been observed. This behaviour marks the beginning of the formation of oxides of iron. The isomer shift, quadrupole splitting and internal magnetic field value of 0.46 mm s^{-1}, 0.80 mm s^{-1} and 480 kOe respectively have been calculated (Table 1). These values are in close agreement with the formation of Fe_3O_4 [40]. Samples which were heated at 350°C showed a simpler Mössbauer spectrum of only six lines (curve (e) in Fig. 2) which were narrower than those of Fe_3O_4. The isomer shift and internal magnetic field were similar to those for γ-Fe_2O_3 [41]. No quadrupole splitting was observed, which is consistent with the cubic symmetry. γ-Fe_2O_3 is a ferrimagnetic compound with a spinel structure, in which iron(III) cations occupy both the tetrahedral (A) and octahedral (B) sites, and is usually assumed to have a collinear magnetic structure consisting of two sublattices.

In the case of sample $FeC_4H_2O_4 \cdot 0.5H_2O$ heated isothermally at 410°C, the Mössbauer spectrum showed a six-line pattern due to magnetic hyperfine splitting (curve (f) in Fig. 2) with the isomer shift, quadrupole splitting and internal magnetic field values of 0.31 mm s^{-1}, 0.20 mm s^{-1} and 512 kOe, respectively. These values are in good agreement with the formation of α-Fe_2O_3 [42, 43]. The crystal structure of α-Fe_2O_3 has been reported to be corundum type (α-Al_2O_3). For α-Fe_2O_3, there is a closed packed oxygen lattice where Fe^{3+} cations occupy the octahedral sites [44]. The compound α-Fe_2O_3 is a magnetically unusual complex, being antiferromagnetic at low temperature, then undergoing a transition above the so called Morrin temperature to a weak ferrimagnetic state, due to spin canting, before becoming paramagnetic at high temperatures [45].

When the reaction is carried out in an atmosphere of static air, the gaseous product acts as a gas buffer for the solid state reaction and some of the reaction is poorly defined. For example the role of water molecules in $FeC_4H_2O_4 \cdot 0.5H_2O$ and the role of atmospheric oxygen in the solid state reaction in static air could be clarified by comparing the different physical properties for the reaction carried out in a dynamic dry nitrogen atmosphere.

The DTA and DTG curves for $FeC_4H_2O_4 \cdot 0.5H_2O$ showed an endothermic peak at 101°C and the TGA curve indicated a mass loss between 70 and 101°C, corresponding to the dehydration of $FeC_4H_2O_4 \cdot 0.5H_2O$ under dry nitrogen atmosphere [24]. The decomposition steps could be seen on DTA and DTG curves at 360°C. The TGA curve showed a continuous mass loss from 242°C until crystallization of Fe_3O_4.

The plot of $\log \sigma$ versus T^{-1} in Fig. 1(b) showed a clear peak at 100°C corresponding to the dehydration step of $FeC_4H_2O_4 \cdot 0.5H_2O$. The IR spectrum of the isothermally heated parent compound in region C showed an increase in the intensity of the Fe–O stretching frequency and a decrease in frequency for the coordinated carboxylate band. The X-ray diffraction revealed that FeO was present in this stage together with some $FeC_4H_2O_4$. A steep increase in σ has been observed in region D corresponding to Fe_3O_4 formed as the final product. The sample thus obtained at 425°C shows a negligible variation in σ with variation of temperature. X-ray diffraction analysis has confirmed the formation of this phase. No line which can be assigned to metallic iron could be detected.

The Mössbauer spectrum of the samples $FeC_4H_2O_4 \cdot 0.5H_2O$ heated isothermally at 110 and 250°C under dry nitrogen atmosphere were quite similar to those in Fig. 2 (curves (a) to (d)) and the spectral parameters are summarized in Table 1. At 425°C the Mössbauer spectra (Fig. 3) consist of two superimposed six-line patterns due to Fe^{3+} (A) and to $Fe^{2+,3+}$ (B). The relative linewidth of both the patterns as well as the somewhat greater broadening of the outer lines are ascribed to impurity and vacancy effects. The excess broadening of the outermost lines of the B-site pattern may also be due to the fact that the electronic interchange of B sites is not extremely fast compared to the ^{57}Fe Larmor frequency. Isomer shift, quadrupole splitting and hyperfine fields are in good agreement with the values reported by Kündig [46].

Thermal decomposition processes of ferrous tartrate one and a half hydrate

Simultaneous TGA, DTA and DTG of $FeC_4H_4O_6 \cdot 1.5H_2O$ under the atmospheres of static air and dynamic dry nitrogen have been reported earlier [25]. DTA gave two endothermic peaks, one at 60°C and the other at 107°C, and two peaks were observed at same temperatures in the DTG curve. TGA showed two regions of mass loss, one up to 75°C corresponding

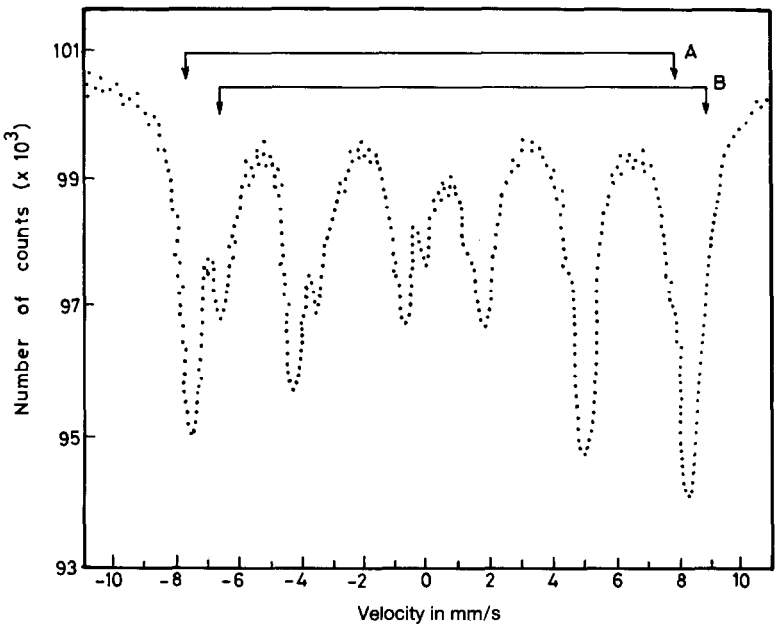

Fig. 3. Room-temperature Mössbauer spectra of the product obtained by heating $FeC_4H_2O_4 \cdot 0.5H_2O$ at 425°C in dry nitrogen atmosphere.

to the loss of half a water molecule, and the other up to 153°C corresponding to the further loss of one water molecule. The oxidative decomposition step for $FeC_4H_4O_6 \cdot 1.5H_2O$ was observed through the presence of a very strong and broad exothermic peak at 209°C in the DTA curve. The DTG curve gave a strong and broad peak at 209°C and the TGA curve showed a continuous mass loss from 160°C until final recrystallization of α-Fe_2O_3 [25].

Region B′ and B″ in the plot of $\log \sigma$ versus T^{-1} shown in Fig. 4(a) corresponds to dehydration of $FeC_4H_4O_6 \cdot 1.5H_2O$ under static atmosphere. There was a steady increase in σ at 153°C followed by another steep increase at 230°C (see regions C and D in Fig. 4(a)). These two temperature ranges (153–228°C and 230–342°C) can be tentatively assigned to the formation of FeO and Fe_3O_4, respectively. However, our repeated experiments to obtain pure FeO by careful heating in static air, even at 210°C, always led to the formation of a mixture of FeO and $FeC_4H_4O_6$. As the X-ray diffraction pattern of the sample obtained in this way showed broad lines, the product seems to be less crystalline. The IR spectrum of a sample heated isothermally in regions C and D showed bands at 396 and 349 cm^{-1}, which are due to Fe–O stretching frequencies. A sample in region E (Fig. 4(a)) was mainly γ-Fe_2O_3 with traces of Fe_3O_4; the X-ray diffraction pattern was generally broad. The temperature range (at about 400°C) of region F corresponded to the complete transformation of γ-Fe_2O_3 to α-Fe_2O_3.

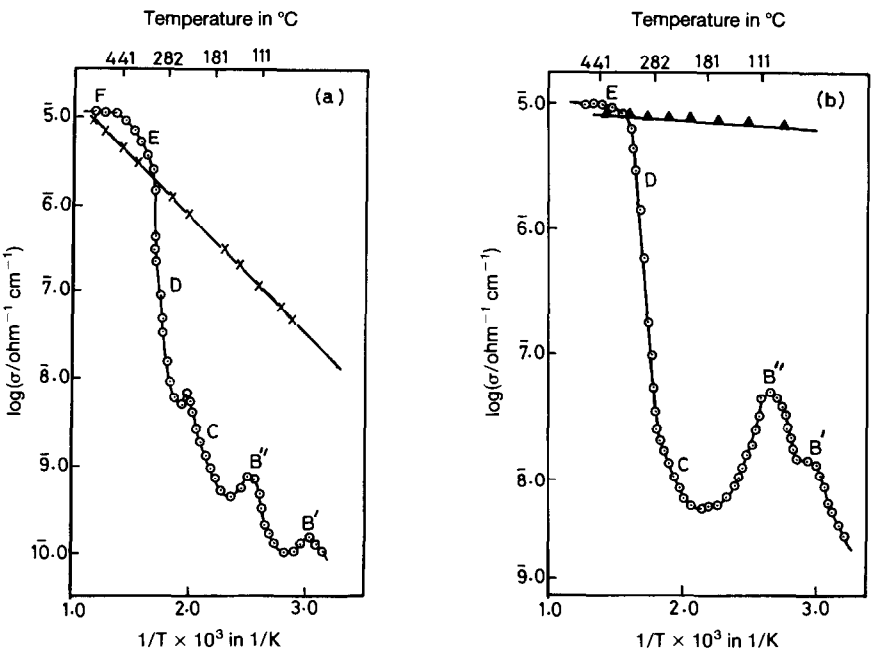

Fig. 4. Plot of $\log \sigma$ vs. T^{-1} for $FeC_4H_4O_6 \cdot 1.5H_2O$ during decomposition in (a) static air and (b) dynamic dry nitrogen atmosphere: ⊙, during decomposition; ×, cooling cycle for α-Fe_2O_3; ▲, cooling cycle for Fe_3O_4.

The Mössbauer spectra of ferrous tartrate one and a half hydrate, monohydrate and anhydrous $FeC_4H_4O_6$ are shown in Fig. 5 and the spectral parameters are summarized in Table 2. The spectrum of the one and a half hydrate (curve (a) in Fig. 5) gave two peaks with almost equivalent intensity, indicating that Fe^{2+} is in one ion site, probably in an octahedral environment. The values of isomer shift and quadrupole splitting were in good agreement with those in the literature [37]. The Mössbauer spectra of anhydrous $FeC_4H_4O_6$ (curve (c) in Fig. 5) showed the larger quadrupole doublet, mainly attributed to the charge distribution in the Fe^{2+} (i.e. more symmetrical). It is well established that the contributions to the electric-field gradient around high-spin Fe(II) from the valence electrons and from surrounding charges are of opposite sign [47]. The spectrum of the monohydrate (curve (b) in Fig. 5) was almost the superposition of those of the original and anhydrous tartrate. This may be an indication that the monohydrate was a mixture of both compounds.

The Mössbauer spectrum of the product at 210°C (curve (d) in Fig. 5) could be assigned to FeO on the basis of the conclusion for ferrous fumarate. The Mössbauer spectrum of the product at 330°C (curve (e) in Fig. 5) is somewhat broad and split, suggesting that the product is a mixture of several compounds. The values of isomer shift, quadrupole splitting and internal magnetic field were near the published data for Fe_3O_4 [40].

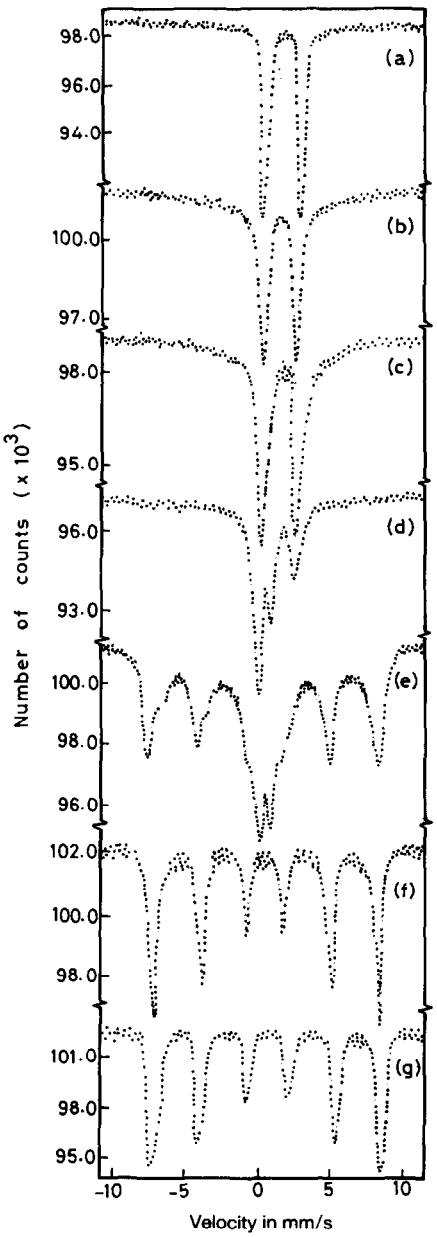

Fig. 5. Room-temperature Mössbauer spectra of (a) $FeC_4H_4O_6 \cdot 1.5H_2O$ and its products at (b) 85°C, (c) 160°C, (d) 210°C, (e) 330°C, (f) 420°C in static air.

The Mössbauer spectrum of $FeC_4H_4O_6 \cdot 1.5H_2O$ heated at 360°C represents a six-line pattern (similar to curve (e) in Fig. 2) with isomer shift, quadrupole splitting and internal magnetic field, indicating the formation of γ-Fe_2O_3 [41]. In the case of sample $FeC_4H_4O_6 \cdot 1.5H_2O$, heated isothermally at 420°C, the Mössbauer spectrum showed a six-line pattern due to

TABLE 2

Mössbauer parameters [a] of $FeC_4H_4O_6 \cdot 1.5H_2O$ and its products at each decomposition stage; Mössbauer measurements were carried out at room temperature (25°C)

Atmosphere	Temperature ranges/°C	Region	Predicted products	Isomer shift/mm s^{-1} [b]	Quadrupole splitting/mm s^{-1} [c]	Internal magnetic field/kOe [d]
Static air	25	A	$FeC_4H_4O_6 \cdot 1.5H_2O$	1.17	2.39	
	50–94	B′	$FeC_4H_4O_6 \cdot H_2O$	1.20	2.48	
	94–160	B″	$FeC_4H_4O_6$	1.30	2.89	
	160–228	C	$FeO + FeC_4H_4O_6$	0.70	0.58	
	228–342	D	Fe_3O_4	0.48	0.85	485
	342–390	E	γ-Fe_2O_3	0.23		494
	Above 400	F	α-Fe_2O_3	0.35	0.23	515
Dynamic dry nitrogen	25	A	$FeC_4H_4O_6 \cdot 1.5H_2O$	1.19	2.37	
	50–115	B′	$FeC_4H_4O_6 \cdot H_2O$	1.21	2.47	
	115–270	B″	$FeC_4H_4O_6$	1.30	2.85	
	270–374	C	$FeO + FeC_4H_4O_6$	0.67	0.63	
	Above 375	D	Fe_3O_4	0.48	0.86	483

[a] With respect to natural iron foil. [b] Values ± 0.02 mm s^{-1}. [c] Values ± 0.03 mm s^{-1}. [d] Values ± 5.0 kOe.

magnetic hyperfine splitting (similar to curve (f) in Fig. 2) with the isomer shift, quadrupole splitting and the internal magnetic field. These values are in good agreement with the formation of α-Fe_2O_3 [42].

In dry nitrogen atmosphere TGA of $FeC_4H_4O_6 \cdot 1.5H_2O$ showed the loss of one and a half water molecules at 120°C, as reported earlier [25]. The DTA curve exhibited a single endothermic peak at 120°C and the DTG curve at 110°C. These thermal curves therefore indicated single step dehydration under this atmosphere. An endothermic peak was observed at 350°C in DTA, with the same on the DTG curve, corresponding to thermal decomposition. TGA shows a continuous mass loss between 250 and 460°C [25].

The plot of log σ versus T^{-1} in Fig. 4(b) indicated that the decomposition of $FeC_4H_4O_6 \cdot 1.5H_2O$ proceeds via the formation of intermediates of varying conductivities, and was quite similar to Fig. 1(b). Here the cooling curve was also recorded, to test the purity of Fe_3O_4 formed. The IR spectrum and X-ray diffraction pattern for samples heated isothermally at 460°C showed pure Fe_3O_4. No line which could be assigned to metallic iron could be detected.

The Mössbauer spectra of the same $FeC_4H_4O_6 \cdot 1.5H_2O$ sample heated isothermally at 200, 320 and 460°C under dry nitrogen atmosphere were quite similar to those of Fig. 5, curves (c) and (d) and Fig. 3 respectively. The isomer shift, quadrupole splitting and internal magnetic field values are given in Table 2 and are in good agreement with the reported value for Fe_3O_4 [46].

The gaseous products obtained by thermal decomposition of $FeC_4H_2O_4 \cdot 0.5H_2O$ under a dynamic pure and dry nitrogen atmosphere are indicated by the gas chromatograms shown in Fig. 6. These chromatograms showed

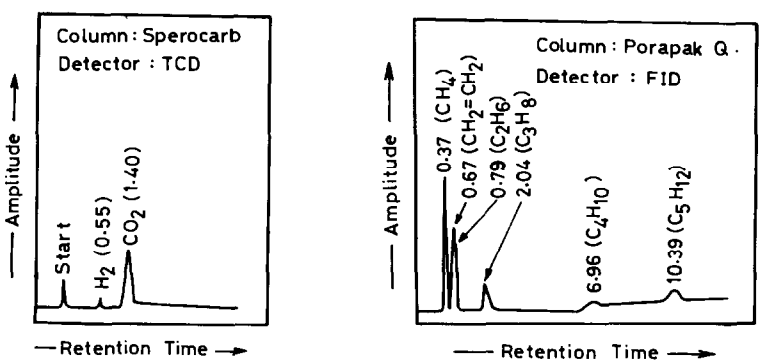

Fig. 6. (a) and (b) Gas–liquid chromatograms for gases obtained during the thermal decomposition of $FeC_4H_2O_4 \cdot 0.5H_2O$ or $FeC_4H_4O_6 \cdot 1.5H_2O$ under dynamic nitrogen atmosphere.

the presence of both types of gases, i.e. polar (H_2, CO_2, etc.) and non-polar (C_2H_2, C_2H_4, etc.) gases. The gases were collected at around 350°C. A similar gas chromatogram was obtained by thermal decomposition of $FeC_4H_4O_6 \cdot 1.5H_2O$ under dry nitrogen atmosphere.

The different paths followed by the decomposition of $FeC_4H_2O_4 \cdot 0.5H_2O$ in different atmospheres showed complete dehydration, as was seen from conductivity measurements, Mössbauer spectra and the IR spectrum. A transformation of $FeC_4H_2O_4$ to FeO was also detected in static and dry nitrogen atmosphere. A separate phase of FeO could be obtained; this compound always occurred with $FeC_4H_2O_4$. Thus the transformation of FeO and $FeC_4H_2O_4$ seems to be an equilibrium reaction. This mixture of FeO and $FeC_4H_2O_4$ is then transformed to Fe_3O_4, which is the final product obtained in dry nitrogen atmosphere.

$$FeC_4H_2O_4 \cdot 0.5H_2O \xrightarrow{65-160°C} FeC_4H_2O_4 + 0.5H_2O(g) \quad (1)$$

$$FeC_4H_2O_4 \xrightarrow{160-280°C} FeO + C_2H_2(g) + CO(g) + CO_2(g) \quad (2)$$

$$2FeO + FeC_4H_2O_4 \xrightarrow{280-440°C} Fe_3O_4 + C_2H_2(g) + 2CO(g) \quad (3)$$

The decomposition paths of $FeC_4H_2O_4 \cdot 0.5H_2O$ in static air were found to be similar except the step for formation of the intermediate γ-Fe_2O_3

$$FeC_4H_2O_4 \cdot 0.5H_2O \xrightarrow{60-160°C} FeC_4H_2O_4 + 0.5H_2O(g) \quad (4)$$

$$FeC_4H_2O_4 \xrightarrow{160-226°C} FeO + C_2H_2(g) + CO(g) + CO_2(g) \quad (5)$$

$$FeO + 2FeC_4H_2O_4 \xrightarrow{226-320°C} Fe_3O_4 + 2C_2H_2(g) + 4CO(g) + [O] \quad (6)$$

$$2Fe_3O_4 + [O] \xrightarrow{320-390°C} 3\gamma\text{-}Fe_2O_3 \quad (7)$$

$$\gamma\text{-}Fe_2O_3 \xrightarrow{390-450°C} \alpha\text{-}Fe_2O_3 \quad (8)$$

Similar reaction paths for $FeC_4H_4O_6 \cdot 1.5H_2O$ were observed in static air and dry nitrogen atmosphere.

CONCLUSIONS

The results of the present study allow us to make the following important observations regarding the solid state decomposition of $FeC_4H_2O_4 \cdot 0.5H_2O$ and $FeC_4H_4O_6 \cdot 1.5H_2O$.

(a) The dehydration of $FeC_4H_2O_4 \cdot 0.5H_2O$ and $FeC_4H_4O_6 \cdot 1.5H_2O$ yielding anhydrous $FeC_4H_2O_4$ or $FeC_4H_4O_6$, took place in static air or dynamic dry nitrogen atmospheres.

(b) The oxidation decomposition behaviour of $FeC_4H_2O_4 \cdot 0.5H_2O$ or $FeC_4H_4O_6 \cdot 1.5H_2O$ was better understood from the study of d.c. electrical

conductivity measurements, which showed different regions of conductivity for the intermediates formed, whereas the oxidative decomposition behaviour could not be clearly understood from the thermal curves.

(c) Mössbauer spectrum of $FeC_4H_2O \cdot 0.5H_2O$ or $FeC_4H_4O_6 \cdot 1.5H_2O$ gave two absorptions with equal width and intensity, indicating that Fe^{2+} is in one ion site, probably in an octahedral environment.

(d) The Mössbauer spectrum of anhydrous fumarate or tartrate showed the larger quadrupole doublet, mainly attributed to the charge distribution in Fe^{2+}.

(e) The Mössbauer spectra of isothermally heated samples of $FeC_4H_2O_4 \cdot 0.5H_2O$ and $FeC_4H_4O_6 \cdot 1.5H_2O$ under static air and dynamic dry nitrogen were comparable, except that the final product obtained in nitrogen atmosphere was Fe_3O_4.

(f) The gas chromatograms showed that both polar and non-polar gases were obtained during thermal decomposition.

ACKNOWLEDGEMENTS

The authors are grateful to the Head, Department of Chemistry, University of Poona, Pune 411 007, for his interest and encouragement. They also thank the Director, National Chemical Laboratory, Pune, India, for facilities given for part of the work.

REFERENCES

1 K.S. Rane, A.K. Nikumbh and A.J. Mukhedkar, J. Mater. Sci., 16 (1981) 2387.
2 K. Seshan, H.R. Anantharaman, Venkatesh Rao, A.L. Shashimohan, H.V. Keer and D.K. Chakraborty, Bull. Mater. Sci., 3 (1981) 201.
3 E.D. Macklen, J. Inorg. Nucl. Chem., 29 (1967) 1229.
4 V. Rao, A.L. Shashimohan and A.B. Biswas, J. Mater. Sci., 9 (1974) 430.
5 M.J. Halsey and A.M. Pritchard, J. Chem. Soc. A, (1968) 2878.
6 R.A. Brown and S.C. Bevan, J. Inorg. Nucl. Chem., 28 (1966) 387.
7 D. Dollimore and D. Nicholson, J. Chem. Soc., (1962) 960.
8 D. Broadbent, D. Dollimore and J. Dollimore, J. Chem. Soc., (1967) 451.
9 G.C. Nicholson, J. Inorg. Nucl. Chem., 29 (1967) 1599.
10 D. Dollimore and D.L. Griffiths, J. Therm. Anal., 2 (1970) 229.
11 F. Lihl, Acta. Phys. Austriaca, 4 (1951) 360.
12 J. Robin and J. Benard, C.R. Acad. Sci., 232 (1951) 1830.
13 P.K. Gallagher and C.R. Kurkjian, Inorg. Chem., 5 (1966) 214.
14 A. Boullé and J.L. Doremieux, C.R. Acad. Sci., 248 (1959) 2211.
15 J.L. Doremieux and A. Boullé, C.R. Acad. Sci., 250 (1960) 3184.
16 E.D. Macklen, J. Inorg. Nucl. Chem., 30 (1968) 2689.
17 D. Dollimore, D.L. Griffiths and D. Nicholson, J. Chem. Soc., (1963) 2617.
18 Ya. A. Ugai, Zh. Obshch. Khim., 24 (1954) 1315.
19 J. Robin, Bull. Soc. Chim. Fr., (1953) 1078.
20 C. Duval, Inorganic Thermogravimetric Analysis, Elsevier, Amsterdam, 1963.
21 F. de S. Barros, P. Zory and L.E. Campbell, Phys. Lett., 7 (1963) 135.
22 P.R. Brady and J.F. Dunacn, J. Chem. Soc., (1964) 653.

23 A.K. Nikumbh, A.E. Athare and V.B. Raut, Thermochim. Acta, 186 (1991) 217.
24 A. Venkataraman, V.A. Mukhedkar, M.M. Rahman, A.K. Nikumbh and A.J. Mukhedkar, Thermochim. Acta, 115 (1987) 215.
25 A. Venkataraman, V.A. Mukhedkar and A.J. Mukhedkar, J. Therm. Anal., 35 (1989) 2115.
26 K. Muraishi, T. Takano and K. Nagase, J. Inorg. Nucl. Chem., 43(10) (1981) 2293.
27 P.S. Bassi, B.S. Randhawa and H.S. Jamwal, Thermochim. Acta, 65 (1983) 1.
28 S. Musić, M. Ristić and S. Popović, J. Radioanal. Nucl. Chem., 121 (1988) 61.
29 M. Ravi and R. Jagannathan, Hyperfine Interaction, 12 (1982) 167.
30 N. Ravi, R. Jagannathan, B.R. Rao and M.R. Hussain, Inorg. Chem., 21 (1982) 1019.
31 C.T. Dziobkowski, J.T. Wrobleski and D.B. Brown, Inorg. Chem., 20 (1981) 671.
32 R. Ramani, M.P. Sathyavathiamma, N.G. Puttaswamy and R.M. Mullya, Proc. Nucl. Phys. Solid State Phys. Symp., 19C (1976) 411.
33 J.A. Jean, I.M. Borrios and S.E. Robles, J. Radioanal. Nucl. Chem., 128 (1988) 139.
34 A.M. Glebov, A.S. Khramov, E.V. Kirillova, Sh. T. Yusupov, Yu. I. Salnikov and Z.N. Yusupov, Zh. Neorg. Khim., 35 (1990) 2290.
35 D.S. Kulgawczuk, K. Ruebenbauer and B. Sepiol, J. Radioanal. Nucl. Chem., 131 (1989), 43.
36 S. Carać, L. Marinkov and J. Slivka, Phys. Status Solidi A, 31 (1975) 263.
37 Y. Takashima and Y. Tateishi, Bull. Chem. Soc. Jpn., 38 (1965) 1688.
38 K. Nakamoto, Infrared Spectra of Inorganic and Coordination Compounds, Wiley Interscience, New York, 2nd edn., 1970, p. 244.
39 D.P. Johnson, Solid State Commun., 7 (1965) 1785.
40 N.N. Greenwood and T.C. Gibb, Mössbauer Spectroscopy, Chapman and Hall, London, 1971, p. 241.
41 D. Khalafalla and A.H. Morrish, J. Appl. Phys., 43 (1972) 624.
42 O.C. Kistner and A.W. Sunyar, Phys. Rev. Lett., 4 (1960) 412.
43 C. Janot and H. Gilbert, Bull. Soc. Fr. Mineral. Crystallogr., 93 (1970) 213.
44 C. Haul and S. Shoon, Z. Phys. Chem., 44 (1939) 216.
45 R.C. Nininger Jr. and D. Shroeer, J. Phys. Chem. Solids, 39 (1978) 137.
46 W. Kündig, Bull. Am. Phys. Soc., 11 (1968) 667.
47 R. Ingalls, Phys. Rev. A., 133 (1964) 787.
48 A.K. Nikumbh, M.M. Phadke and A.A. Latkar, J. Magn. Magn. Mater., 131 (1994) 189.